Heat-flow equation motivated by the ideal-gas shock wave

Brad Lee Holian[1] and Michel Mareschal[2]
[1]*Theoretical Division, Los Alamos National Laboratory, Los Alamos, New Mexico 87545, USA*
[2]*Physics Department, CP223, Université Libre de Bruxelles, B-1050 Bruxelles, Belgium*
(Received 29 October 2009; revised manuscript received 22 July 2010; published 31 August 2010)

We present an equation for the heat-flux vector that goes beyond Fourier's Law of heat conduction, in order to model shockwave propagation in gases. Our approach is motivated by the observation of a disequilibrium among the three components of temperature, namely, the difference between the temperature component in the direction of a planar shock wave, versus those in the transverse directions. This difference is most prominent near the shock front. We test our heat-flow equation for the case of strong shock waves in the ideal gas, which has been studied in the past and compared to Navier-Stokes solutions. The new heat-flow treatment improves the agreement with nonequilibrium molecular-dynamics simulations of hard spheres under strong shockwave conditions.

DOI: 10.1103/PhysRevE.82.026707 PACS number(s): 47.11.Mn, 02.70.Ns, 45.10.−b

I. INTRODUCTION

Previous studies of planar shock waves in the ideal gas have proven to be helpful in the fundamental understanding of the continuum equations of change in hydrodynamics. The earliest work of Mott-Smith proposed that the shock wave would exhibit differences among the three components of temperature, i.e., that the temperature component measured in the shock direction would exceed that of the other transverse directions, due to a bimodal distribution of temperatures [1,2]. Later work, motivated by atomistic nonequilibrium molecular-dynamics (NEMD) computer simulations of moderate and strong shock waves in dense fluids, showed that the usual description of the constitutive equations governing shear flow (Navier-Stokes) and heat transport (Fourier's Law), do an adequate job of describing shockwave profiles [3–6].

Profiles of the hydrodynamic variables as functions of distance along the shock direction x can be constructed from these simulations: density ρ, particle velocity u, pressure-tensor components P_{xx} (along the shock direction) and $P_{zz}=P_{yy}$ (in the transverse directions), and internal energy per unit mass E. Though the temperature is not directly determined in a shock wave, we will show how to obtain profiles of the directional components of the kinetic temperature tensor: T_{xx} along the shock direction and $T_{zz}=T_{yy}$ in the transverse directions; one-third the trace of the kinetic temperature tensor is usually referred to as simply "the temperature," T, and we will continue to honor that practice, though keeping in mind that T_{xx} departs markedly from T in the vicinity of the shockwave front, indicating a strong anisotropy in the velocity distribution function.

The linear NS (and Fourier) constitutive "laws" of viscous flow and thermal conduction relate fluxes of momentum P_{xx} and energy Q to the gradients of velocity du/dx and temperature dT/dx, respectively, through the transport coefficients of viscosity—bulk η_V and shear η_S—and thermal conductivity κ, thereby augmenting the equilibrium equation of state (EOS) that gives the energy and pressure as functions of density and temperature. The transport coefficients are also functions of density and temperature.

For strong shock waves in the ideal gas, it was found that the NS constitutive laws predicted narrower shock profiles than were observed in NEMD simulations [7]. Later, it was proposed that the temperature dependence of the transport coefficients could be improved by exchanging the longitudinal temperature T_{xx} for the average temperature T [8]. Since the ideal-gas transport coefficients depend on the square root of temperature, they are enhanced by the use of T_{xx}, which is larger than T in a shock wave; therefore, the increased dissipation broadens the shock width, in agreement with the NEMD simulations. Nevertheless, the NEMD shock width is even greater than predicted by NS with this T_{xx} augmentation of the transport coefficients—so-called "NSx." The result is that there is additional dissipation required, over and above this NSx level. (Kum *et al.* [9] also noted in subsequent work that two-dimensional fluid shock waves exhibit temperature maxima and that NS theory does not describe adequately all aspects of the profiles they observed.)

For that reason, we propose an equation for the heat-flux vector Q, going beyond Fourier's Law. While the motivation to generalize heat conduction to deal with strong shock lies in the direct observations from NEMD simulations, our aim is to remain, as much as possible, at a macroscopic level with recourse neither to higher-order expansion of fluxes in the gradients nor sophisticated Boltzmann-equation solution methods, such as Mott-Smith [1]. The basic idea is to allow for differences in T_{xx} and T, and to supplement the description with an equation for relaxing the nonequipartition of kinetic energy between T_{xx} and T.

As the shock strength becomes larger, deviations from local equilibrium increase, as shown in the differences between the temperatures computed in the various directions: for weak shocks this temperature-difference relaxation can be described by viscous shear dissipation. For stronger shocks, however, NEMD simulations show that more dissipation is needed. What we propose is to add an additional relaxation term in the constitutive relation for the heat flux, as is done in the Cattaneo equation (or telegrapher's equation). This term is known to be relevant whenever the ratio of the collision time to the hydrodynamic time cannot be neglected. This is the case inside the shock front where the

heat-flux variations take place on a few mean free paths, or alternatively in a few collision times.

The description proposed is inspired by the work of Cattaneo [11] who was motivated by describing finite speed heat transport: since then, similar formulations have been applied to a wide variety of problems (see for example the review of Ref. [11]). In approaches of this kind, the description goes beyond local equilibrium thermodynamics, as would be obtained, for example, in the first order of a gradient expansion of kinetic-theory solutions. Therefore, the set of macroscopic variables needed to describe the strong shock front does not simply extend equilibrium concepts to nonequilibrium states. This is usual whenever first-order gradient expansions are not sufficient to account for observed phenomena: theories become nonlinear and lose equilibrium-inspired simplicity and symmetry [15]. Those are recovered, however, with the decrease of shock strength.

After presenting those ideas in more detail within the context of strong shock waves in gases, we compare the continuum theories with atomistic NEMD results. For the ideal gas, the EOS and transport coefficients are simple analytic functions of density and temperature, but numerical integration of the profiles is nevertheless necessary. Remarkably, the HM prediction of the shock width and the magnitude of the heat-flux vector are in much better agreement with NEMD than NS.

II. SOLVING CONTINUUM EQUATIONS FOR THE STEADY, PLANAR SHOCK WAVE

Consider a left-moving piston (velocity $-u_p$) that generates a planar shock wave (velocity $-u_s$) in the x direction into an ideal gas that is initially stationary [10]. The shock front separates the initial state (mass density ρ_0, particle velocity $u=0$, pressure P_0, energy E_0, and temperature T_0) from the final state $(\rho_1, u=-u_p, P_1, E_1, T_1)$. Moving in the frame of reference of the shock front, i.e., by adding $+u_s$ to all velocities, the cold material streams in from the left at $+u_s$, the shock front is stationary at $x=0$, and the piston recedes to the right at velocity u_s-u_p, with hot material stagnating against the rightward-moving piston. In this frame of reference, where the shockwave profile is steady in time, conservation of mass, momentum, and energy are represented by constant fluxes (in each case, the first equality is for the cold side; the second is for the hot, dense, high-pressure side),

$$\rho u = \rho_0 u_s = \rho_1 (u_s - u_p) \Rightarrow \rho = \frac{\rho_0 u_s}{u}, \tag{1}$$

where the volumetric strain $\varepsilon = V/V_0 - 1 = \rho_0/\rho_1 - 1$ (the volume per unit mass $V = 1/\rho$ and the final strain in the shocked state is $\varepsilon_1 = -u_p/u_s$);

$$P_{xx} + \rho u^2 = P_0 + \rho_0 u_s^2 = P_1 + \rho_1 (u_s - u_p)^2, \tag{2}$$

where P_{xx} is the longitudinal component of the pressure tensor in the shock (x) direction;

$$\begin{aligned} \rho u\left(E + \frac{1}{2}u^2 + \frac{P_{xx}}{\rho}\right) + Q &= \rho_0 u_s\left(E_0 + \frac{1}{2}u_s^2 + \frac{P_0}{\rho_0}\right) \\ &= \rho_1 (u_s - u_p)\left[E_1 + \frac{1}{2}(u_s - u_p)^2 + \frac{P_1}{\rho_1}\right], \end{aligned} \tag{3}$$

where E is the internal energy per unit mass, and Q is the heat-flux vector (zero in both cold and hot equilibrium states far from the shock front),

$$\begin{aligned} \frac{Q}{\rho_0 u_s} &= E_0 - E + \frac{1}{2}(u_s^2 - u^2) + \frac{P_0}{\rho_0} - \frac{P_{xx}}{\rho} \\ &= E_0 - E + \frac{1}{2}(u_s - u)^2 + \frac{P_0}{\rho_0}\left(1 - \frac{u}{u_s}\right), \end{aligned} \tag{4}$$

which has been further simplified in the second line by using the earlier flux equations. Likewise, we can express the momentum-conservation condition more simply as

$$P_{xx} = P_0 + \rho_0 u_s (u_s - u) \Rightarrow P_1 = P_0 + \rho_0 u_s u_p, \tag{5}$$

which demonstrates the Hugoniot condition for the final pressure rise through the shock. The Hugoniot condition for the final energy rise through the shock is obtained from Eq. (4), where $E=E_1$, $u=u_s-u_p$, and $Q=0$,

$$E_1 = E_0 + \frac{P_0}{\rho_0}\frac{u_p}{u_s} + \frac{1}{2}u_p^2 = E_0 + \frac{1}{2}(P_1 + P_0)(V_0 - V_1). \tag{6}$$

The second equality expresses the triangular area under the Rayleigh line in the P-V diagram, namely, the PV work done by the shockwave process.

There are two Navier-Stokes (NS) constitutive relations for the shock process: viscous flow (a longitudinal combination of viscosities, bulk η_V, and shear η_S) for the longitudinal component of the pressure tensor P_{xx} and Fourier's Law of heat flow for the heat-flux vector Q. The hydrostatic pressure exceeds the equilibrium pressure P from the EOS, since the volumetric strain rate $\dot{\varepsilon} = du/dx \leq 0$ (in compression),

$$\bar{P} = \frac{1}{3}(P_{xx} + 2P_{yy}) = P(\rho, T) - \eta_V(\rho, T)\dot{\varepsilon}. \tag{7a}$$

The shear stress is given by half the normal-pressure difference $P_{xx}-P_{yy}$,

$$\tau = \frac{1}{2}(P_{xx} - P_{yy}) = -\eta_S(\rho, T)\dot{\varepsilon}, \tag{7b}$$

which is greater than zero in compression. Hence, the longitudinal pressure-tensor component throughout the shockwave profile exceeds the equilibrium pressure P from the EOS (the longitudinal viscosity is η_L),

$$P_{xx} = \bar{P} + \frac{4}{3}\tau = P(\rho, T) - \eta_L(\rho, T)\dot{\varepsilon}, \quad \eta_L = \eta_V + \frac{4}{3}\eta_S. \tag{7c}$$

The corresponding components of the kinetic temperature tensor are similarly given by

$$\bar{T} = \frac{1}{3}(T_{xx} + 2T_{yy}) = T,$$

$$T_{sh} = \frac{1}{2}(T_{xx} - T_{yy}),$$

$$T_{xx} = T + \frac{4}{3}T_{sh}. \tag{8}$$

Note, however, that there is no distinction between the temperature and one-third the trace of the kinetic temperature tensor, as there is between the equilibrium pressure from the EOS and one-third the trace of the pressure tensor: in other words, there is no kinetic equivalent to the bulk viscosity, which depends entirely upon potential contributions and is zero for the ideal gas.

It is worth mentioning that those temperature variables and their properties appear naturally in a kinetic-theory context (see Ref. [2]); their interpretation in terms of a parameter characteristic of the distribution of peculiar particle velocities (i.e., velocities with respect to the local fluid velocity) provide us with a simple physical meaning: it also brings evidence that those definitions are independent of a particular geometry or frame of reference.

The alert reader may have noticed by now that Navier-Stokes uses the common assumption of local thermodynamic equilibrium; the EOS and transport properties are specified as functions of ρ and T, which are determined throughout the shockwave profile as functions of the profile coordinate x. No mention is made of the truly nonequilibrium variable T_{xx}, the temperature in the direction of the shock that arises from rapid uniaxial compression. How, you may well ask, is T_{xx} supposed to be determined in a continuum theory? In molecular-dynamics simulations, of course, T_{xx} can be calculated explicitly from particle coordinates and velocities. In the case of the ideal gas, the pressure tensor is the product of density and the temperature tensor: the relationship is straightforward since there is no potential part of the pressure tensor to contend with.

The Navier-Stokes constitutive equation for heat flow is Fourier's Law of thermal conduction for the heat-flux vector,

$$Q_0 = -\kappa(\rho,T)\frac{dT}{dx}, \tag{9}$$

where κ is the NS thermal conductivity that depends only on the density and average temperature. The heat flow predicted by NS in shock waves is insufficient to explain the observed shock thickness in NEMD shock simulations. In earlier work, we proposed to include the longitudinal temperature, rather than the average temperature in the transport coefficients, but while that modification was an improvement over NS, it was not entirely successful when compared to NEMD results [8]. Moreover, such a modification does not really address the relaxation process of the temperature components in the shock front.

In order to describe the relaxation of the kinetic temperature tensor components in the shock wave, Fourier's Law can be extended to include a microscopic relaxation process, using the Cattaneo (also known as the telegrapher's) equation [11],

$$Q + \tau_c\frac{\partial Q}{\partial t} = Q_0 = -\kappa\frac{\partial T}{\partial x}, \tag{10a}$$

whose formal solution can be written as the Maxwell (exponential) relaxation equation,

$$\frac{\partial Q}{\partial t} = -\frac{Q - Q_0}{\tau_c}, \tag{10b}$$

where τ_c is a characteristic microscopic relaxation time (such as the mean collision time). From Eq. (4), we have that the isotropic Q_0 is defined to be

$$\frac{Q_0}{\rho_0 u_s} = E_0 - E(\rho,T) + \frac{1}{2}(u_s^2 - u^2) + \frac{P_0}{\rho_0} - \frac{P(\rho,T)}{\rho}, \tag{10c}$$

so that we see that the contribution to the heat-flux vector made by the relaxation of the normal component of the pressure tensor P_{xx} toward the equilibrium pressure $P(\rho,T)$ gives

$$Q - Q_0 = -\rho u\frac{P_{xx} - P}{\rho} = -(P_{xx} - P)u = \eta_L\dot{\varepsilon}u, \tag{10d}$$

where the final equality follows from Eq. (7c). Hence, Eq. (10a) for the steady shock wave becomes

$$Q = -\kappa\frac{dT}{dx} + \delta_2\eta_L\frac{du}{dx}u. \tag{11a}$$

This shows that, in the steady planar shock wave, the nonequilibrium relaxation of the longitudinal kinetic temperature T_{xx} toward its average value T increases the (negative) magnitude of the heat-flux vector, over and above that from Fourier's Law. The shock wave is characterized by a nonequilibrium velocity distribution function that is highly anisotropic (cigar-shaped in the direction of shock propagation) at the front of the shock, which relaxes toward a spherical Maxwell-Boltzmann distribution after the shock wave has passed. The dimensionless parameter δ_2 governs the strength of the relaxation process; for NS, it is zero, but in general, it is a number less than one, as we will show.

We can generalize the conductivity in Eq. (11a) to include a nonlinear dependence on the strain rate, over and above the NS value,

$$\bar{\kappa}(\rho,T;\dot{\varepsilon}) = \kappa(\rho,T)[1 - \delta_1\dot{\varepsilon}\tau_c(\rho,T)], \tag{11b}$$

which introduces a term in Q that is second order in gradients, reminiscent of the most important higher-order term in the Burnett expansion beyond NS [12,13]. The constant δ_1 is a dimensionless, positive number. In the section on results from NEMD, we will show that this enhancement improves the continuum prediction of the shockwave thickness.

III. IDEAL-GAS EQUATION OF STATE AND TRANSPORT COEFFICIENTS

The equation of state for the ideal gas is

$$E = \frac{3}{2}\frac{kT}{m}, \quad P = \rho\frac{kT}{m}. \tag{12}$$

For the ideal gas of hard spheres [12] of diameter σ and mass m, the bulk viscosity is zero, and the shear viscosity, which depends only on temperature, not density, is given by

$$\eta_S(\rho,T) = \frac{5m}{16\sigma^2}\sqrt{\frac{kT}{\pi m}} \Rightarrow \eta_L = \rho_0 \ell_0^0 \sqrt{\frac{kT}{m}},$$

$$\ell_0^0 = \frac{5m}{12\rho_0\sigma^2\sqrt{\pi}}, \tag{13a}$$

where this convenient scaling parameter ℓ_0^0 is very close to the mean free path in the initial state (which depends only on density, and not on temperature),

$$\ell_0 = \frac{m}{\sqrt{2}\rho_0\pi\sigma^2} \Rightarrow \ell_0^0 = \frac{5}{12}\sqrt{2\pi}\ell_0 \cong 1.044\ell_0. \tag{13b}$$

The mean collision time that corresponds to the mean free path ℓ is $\tau_c = \ell/\bar{c}$, where $\bar{c}$ is the average thermal speed $\sqrt{(8kT/\pi m)}$,

$$\tau_c = \frac{\sigma}{4\sqrt{\pi}}\frac{m}{\rho\sigma^3}\sqrt{\frac{m}{kT}}. \tag{13c}$$

And finally, the ideal-gas thermal conductivity is

$$\kappa(\rho,T) = \frac{75k}{64\sigma^2}\sqrt{\frac{kT}{\pi m}} = \frac{45k}{16m}\eta_L. \tag{13d}$$

It is useful to scale the shock profile variables: the fluid velocity, when scaled by shock velocity, is the scaled volume per unit mass, so that the scaled density is inherently the inverse of velocity, as seen in Eq. (1),

$$v = \frac{u}{u_s} = \frac{V}{V_0} = \frac{\rho_0}{\rho}, \quad \varepsilon = v - 1. \tag{14}$$

The scaled temperature, energy, and pressure become

$$t = \frac{kT}{mu_s^2}, \quad e = \frac{E}{u_s^2}, \quad p = \frac{P}{\rho_0 u_s^2}. \tag{15}$$

The longitudinal component of the pressure tensor from Eq. (5) is then

$$p_{xx} = p_0 + 1 - v = p_0 - \varepsilon. \tag{16}$$

From Eq. (4), the scaled heat-flux vector becomes

$$q = \frac{Q}{\rho_0 u_s^3} = e_0 - e - p_0\varepsilon + \frac{1}{2}\varepsilon^2$$

$$= e_0 - e + p_0(1-v) + \frac{1}{2}(1-v)^2. \tag{17}$$

Finally, when the scaled x coordinate in the direction of shock propagation is χ, the scaled gradients of velocity v' and temperature t' that appear in NS and Fourier are

$$\dot{\varepsilon} = \frac{du}{dx}, \quad \chi = \frac{x}{\ell_0^0}, \quad \dot{\varepsilon} = \frac{u_s}{\ell_0^0}\frac{dv}{d\chi} = \frac{u_s}{\ell_0^0}v',$$

$$\frac{dT}{dx} = \frac{mu_s^2}{k\ell_0^0}\frac{dt}{d\chi} = \frac{mu_s^2}{k\ell_0^0}t'. \tag{18}$$

Now, remembering that $v_0 = 1$, we can write the scaled NS constitutive equation [Eq. (16))] for the case of the ideal gas,

$$p_{xx} = \frac{t_{xx}}{v} = t_0 + 1 - v = \frac{t}{v} - \frac{\eta_L}{\rho_0 u_s \ell_0^0}v'$$

$$= \frac{t}{v} - \sqrt{t}v' \Rightarrow v' = -\frac{t_{xx} - t}{v\sqrt{t}}, \tag{19}$$

and the scaled version of Fourier's Law from Eqs. (9) and (18), using Eq. (17) to express q for the case of the ideal gas,

$$q = \frac{3}{2}(t_0 - t) + t_0(1-v) + \frac{1}{2}(1-v)^2$$

$$= -\frac{\kappa m}{\rho_0 u_s k \ell_0^0}t' = -\frac{45}{16}\sqrt{t}t' \Rightarrow t' = -\frac{q}{\frac{45}{16}\sqrt{t}}. \tag{20a}$$

(At the so-called NSx level, $\sqrt{t_{xx}}$ is substituted above for the $\sqrt{t}$ dependence of the longitudinal viscosity, the thermal conductivity, and the mean collision time.) With the help of Eqs. (13c) and (18), the scaled version of Eq. (11) for our new relaxation and Burnett generalization of the heat flux becomes

$$q = -\frac{45}{16}\sqrt{t}\left[1 + \frac{3}{5}\delta_1\left(\frac{t_{xx}}{t} - 1\right)\right]t' - \delta_2(t_{xx} - t)$$

$$\Rightarrow t' = -\frac{q + \delta_2(t_{xx} - t)}{\frac{45}{16}\sqrt{t}\left[1 + \frac{3}{5}\delta_1\left(\frac{t_{xx}}{t} - 1\right)\right]}. \tag{20b}$$

When the two parameters $\delta_1 = \delta_2 = 0$, Fourier's Law [Eq. (20a)] is recovered from Eq. (20b).

We see from Eq. (19) that the longitudinal temperature t_{xx} is entirely determined by the velocity (or volume) v,

$$t_{xx} = t_0 v + v(1-v). \tag{21}$$

Thus, we can conclude that t_{xx} is mainly due to the uniaxial compression of the shock wave, and is therefore distinct from the temperature t. From Eq. (19), it is clear that since the strain rate in compression is negative ($v' \le 0$), $t_{xx} \ge t$. Moreover, Eq. (21) demonstrates that t_{xx} exhibits a peak in the vicinity of the shock front.

From the Hugoniot jump condition for the energy for strong shocks ($P_0 = 0 = E_0 = T_0$), we see from Eq. (6) that

$$e_1 = \frac{3}{2}t_1 = \frac{1}{2}\varepsilon^2$$

$$\Rightarrow 3t_1 = 3t_{xx}^{(1)} = 3v_1(1-v_1) = v_p^2 = (1-v_1)^2$$

$$\Rightarrow v_1 = \frac{1}{4}, \quad \rho_1 = 4\rho_0, \quad u_s = \frac{4}{3}u_p, \quad t_1 = \frac{3}{16}. \tag{22}$$

Usually, the relationship between shock and piston velocity is written $u_s = c_0 + su_p$; for the ideal gas, $c_0 = 0$ and $s = 4/3$. Notice that, from Eq. (21), at the scaled particle velocity $v = 1/2$, the peak in $t_{xx} = 1/4 = (4/3)t_1$ serves to define the location of the shock front.

To get the continuum theory shockwave profiles as functions of the reduced x-coordinate χ, we integrate Eq. (19) to get the particle velocity v and Eq. (20) to get the temperature t. We have to begin the integration at the hot end, where the piston initiates and supports the shock wave. The equations can be solved by first-order finite differences, with the integration step $d\chi$ negative.

The initial conditions for the strong shock are $t_1 = 3/16$ and $v_1 = 1/4$. We found that starting at $\chi = 2$, with $d\chi = -10^{-4}$ and $v = v_1 + 10^{-6}$, gives sufficient accuracy; the unshocked state, to which the solution tends, is characterized by $t_0 = 0$. We identify the origin of the steady shock front with the maximum of $t_{xx} = 1/4 = (4/3)t_1$, where the particle velocity $v = 1/2$, and shift the origins of the various profiles accordingly. Since the velocity profile is not really symmetric, this fiducial mark occurs much closer to the maximum in the strain rate than the halfway point between cold and hot particle velocities, another common choice for the origin. Moreover, this point in the shockwave profile is common to all levels of approximation for strong shock waves in the ideal gas, since it is a symmetry point of the mass and momentum fluxes.

IV. RESULTS

The modifications we have proposed for the heat-flow equation—nonlinearity in the conductivity and temperature relaxation—reduce the gradient of temperature from its Fourier-Law value, leading to a wider shock wave, in much closer agreement with nonequilibrium molecular-dynamics (NEMD) simulations of strong shocks in the ideal gas. The new relaxation term in the heat-flux vector is motivated by the need to convert the mechanical "temperature" T_{xx} into its transverse brethren T_{yy} and T_{zz} in the course of collisions near the shock front. This transport mechanism operates in the process of uniaxial planar shock waves, and not in the usual flow of heat from a hot body to a cold one, since the shock wave is unique in its capability to generate longitudinal-to-transverse disequilibrium in the momentum distribution.

The zeroth-order Navier-Stokes (NS) solutions for the average temperature and the component of temperature in the shockwave direction are shown in Fig. 1 as functions of the scaled coordinate, as well as the so-called NSx theory [8], where the T-dependence in the transport coefficients is replaced by T_{xx}. Then, the HM heat-flux vector modifications are presented, beginning with only the temperature relaxation contribution, and then adding the Burnett-like nonlinearity (strain-rate dependence) to the conductivity. These continuum theories are compared with (NEMD) simulations of strong shocks in the hard-sphere ideal gas, such as described in Ref. [7].

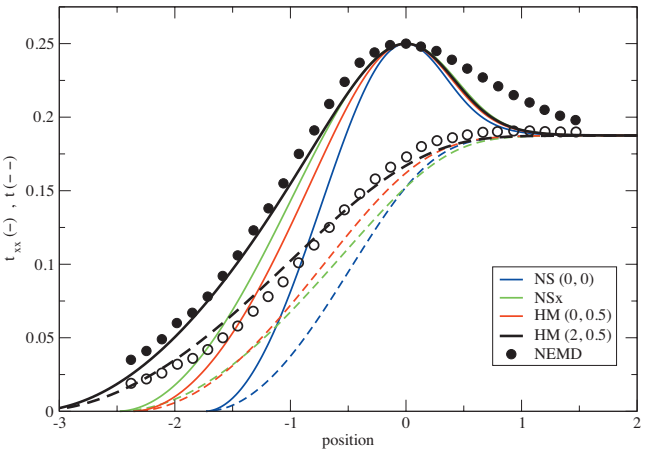

FIG. 1. (Color) Temperature profiles (functions of position) for shock waves in the ideal gas; t is the average temperature (dashed lines, open circles), t_{xx} is the component in the direction of the shock wave (solid lines and circles). The maximum value of t_{xx} marks the common origin of the shock front for all curves; $t_1 = 0.1875$ is the final temperature of the gas at the hot end near the piston (far right-hand side); initial temperature at the cold end (left-hand side) is zero. Nonequilibrium molecular-dynamics (NEMD) simulation data points are for the ideal-gas limit of hard spheres in three dimensions [7]. NS=Navier-Stokes-Fourier ($\delta_1 = \delta_2 = 0$) (blue or thin black), NSx=NS with t-dependence of transport coefficients replaced by t_{xx} (green or light gray), HM (0,0.5) is Holian-Mareschal heat-flux equation [Eq. (11)] with temperature relaxation only (red or gray), and HM (2,0.5) includes nonlinear Burnett conductivity as well as relaxation (thick black).

Note that as we progress in complexity from NS to relaxation only, to relaxation with Burnett-like nonlinearity of the conductivity, the shockwave thickness increases, and the curves approach NEMD more closely. As we stated earlier, the NSx modification is an improvement over NS, but does not match NEMD nearly as well as the HM theory.

Finally, we show in Fig. 2 the heat-flux vector for Navier-Stokes-Fourier, the NSx version, our HM modification to Fourier's Law, and NEMD simulations. Since the position (x axis) in all our figures corresponds to time for a mass element being shocked, the maxima in the magnitude of the gradients of velocity and temperature occur *before* the maxima in the magnitude of their corresponding fluxes (shear stress and heat-flux vector, respectively); that there is a lag time between cause and effect is a feature common to NS, HM, and NEMD. (This is also discussed in Ref. [14] for shock waves in a two-dimensional fluid of soft particles.) The excellent agreement between HM and NEMD demonstrates that incorporating the two effects, namely, nonlinearity and relaxation of the temperature differences between normal and transverse components, is essential for a complete understanding of the thermal effects in shock waves.

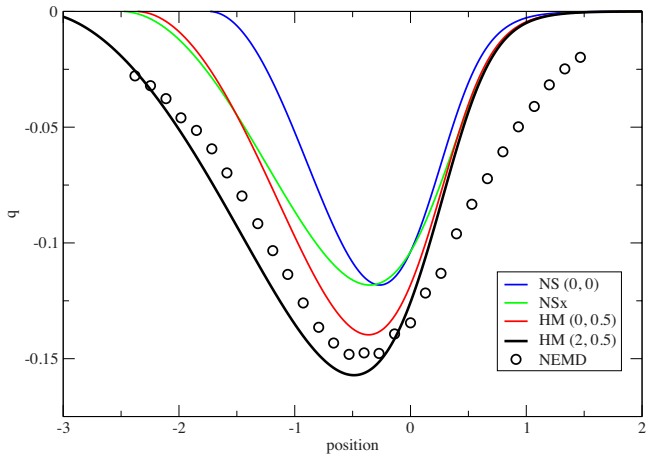

FIG. 2. (Color online) Heat-flux vector profile for a shock wave in the ideal gas. NS=Navier-Stokes-Fourier (blue or thin black), NSx=NS (green or light gray) with t-dependence of transport coefficients replaced by t_{xx}, HM (red or gray, and and thick black) as in Fig. 1, NEMD=nonequilibrium molecular-dynamics simulations. The maximum (negative) magnitude of the heat flux occurs on the cold side of the shock front (i.e., farther from the piston), but the position and magnitude of the NEMD data are more closely matched by HM than by either NS or NSx.

On the other hand, the profiles on the hot side of the shock front show that further improvement is possible, but may be indications of yet other mechanisms of relaxation or higher-order terms in the hydrodynamic description.

V. CONCLUSION

We have presented a heat-flux equation Eq. (11) [in scaled form, Eq. (20)], motivated by nonequilibrium molecular-dynamics simulations in the ideal-gas regime, that goes beyond Navier-Stokes, and improves the agreement between theory and computer experiments, particularly in its better prediction of the shockwave thickness.

In the case of dilute gases, kinetic theory is also successful in predicting features we are dealing with in this paper, in particular Mott-Smith types of solutions of the Boltzmann equation [2]. Our approach remains [with the noticeable exception of Eq. (10)] at a macroscopic level: we want to identify the proper generalization of Fourier's law required for describing strong shocks. In preliminary work, we have shown that similar mechanisms can also be observed in condensed materials, namely, dense fluids, where the continuum prediction of T_{xx} is much more challenging than the dilute gas case.

The two essential ingredients we have used in our approach are (1) to consider two temperatures in the set of state variables, given the observed important departure from equipartition of energy, and (2) to add a (microscopic) relaxation equation for the temperature difference on the scale of a mean free time, making use of the formalism of the Cattaneo equation. We make no claim of generality beyond the case of strong shock waves.

This is rather surprising from the point of view of the usual picture of nonequilibrium transport of heat, but then the shock wave presents new nonequilibrium features not seen in other steady-state situations.

ACKNOWLEDGMENTS

Shock waves, particularly weak ones, often exhibit potential contributions to pressures and energies that far outweigh the kinetic (thermal) parts, so that shocks in the ideal gas, where potential contributions are zero, afford a unique theoretical probe of thermal transport processes. We thank Bill Hoover, a pioneer in atomistic shockwave studies, for inspiring us to revisit our earlier work on the subject of temperatures and heat flow in shock fronts.

[1] H. M. Mott-Smith, Phys. Rev. **82**, 885 (1951).
[2] C. Cercignani, *Rarefied Gas Dynamics: From Basic Concepts to Actual Calculations* (Cambridge University Press, Cambridge, England, 2000) presents an excellent account of kinetic theory of shock waves; Most recent papers are to be found in: Rarefied Gas Dynamics, *Proceedings of the 26th International Symposium on Rarefied Gas Dynamics*, AIP Conference Proceedings (Springer, Melville, NY, 2009), Vol. 1084.
[3] V. Y. Klimenko and A. N. Dremin, in *Detonatsyia Chernogolovka*, edited by O. N. Breusov *et al.* (Akademik Nauk, Moscow, 1978), p. 79.
[4] W. G. Hoover, Phys. Rev. Lett. **42**, 1531 (1979).
[5] B. L. Holian, W. G. Hoover, B. Moran, and G. K. Straub, Phys. Rev. A **22**, 2798 (1980).
[6] W. G. Hoover and C. G. Hoover, Phys. Rev. E **80**, 011128 (2009).
[7] E. Salomons and M. Mareschal, Phys. Rev. Lett. **69**, 269 (1992).
[8] B. L. Holian, C. W. Patterson, M. Mareschal, and E. Salomons, Phys. Rev. E **47**, R24 (1993).
[9] O. Kum, Wm. G. Hoover, and C. G. Hoover, Phys. Rev. E **56**, 462 (1997).
[10] L. D. Landau and E. M. Lifshitz, *Fluid Mechanics* (Reed Publishing, Oxford, 2000).
[11] C. R. Cattaneo, C. R. Hebd. Seances Acad. Sci. **247**, 431 (1958); for a review, see D. D. Joseph and L. Preziosi, Rev. Mod. Phys. **61**, 41 (1989); **62**, 375 (1990); Galilean invariance's property of Cattaneo's equation is discussed in C. I. Christov and P. M. Jordan, Phys. Rev. Lett. **94**, 154301 (2005).
[12] P. Résibois and M. De Leener, *Classical Kinetic Theory of Fluids* (John Wiley-Interscience, New York, 1977).
[13] C. S. Wang Chang and G. E. Uhlenbeck, in *Studies in Statistical Mechanics*, edited by J. de Boer and G. E. Uhlenbeck (North-Holland, Amsterdam, 1970), Vol. 5.
[14] W. G. Hoover and C. G. Hoover, e-print arXiv:0909.2882.
[15] S. R. De Groot and P. Mazur, *Non-equilibrium Thermodynamics* (North-Holland Publishing, Amsterdam, 1962). In particular, Chapter 9 discusses deviations from local equilibrium from kinetic-theory perturbative solutions.